SJIF Impact Factor (2024): 8.675| ISI I.F. Value: 1.241| Journal DOI: 10.36713/epra2016 ISSN: 2455-7838(Online)
EPRA International Journal of Research and Development (IJRD)
Volume: 9 | Issue: 4 | April 2024 - Peer Reviewed Journal

ENHANCING UNDERWATER IMAGE QUALITY THROUGH ADAPTIVE COLOR CORRECTION AND MULTI-SCALE HISTOGRAM EQUALIZATION

Mr.T.Sreedhar[1], B.Ajay Jeevith Kumar[2], P.Venkateswarlu[3], G.Bhargav Vamsi[4], U.Venkata Manikanta[5]

[1] *M.Tech,(Ph.D),Assistant Professor, Dept. of Electronics and Communication Engineering, Usha Rama College of Engineering and Technology, AP, India.*

[2] *B.Tech, Student, Dept. of Electronics and Communication Engineering, Usha Rama College of Engineering and Technology, AP, India.*

[3] *B.Tech, Student, Dept. of Electronics and Communication Engineering, Usha Rama College of Engineering and Technology, AP, India.*

[4] *B.Tech, Student, Dept. of Electronics and Communication Engineering, Usha Rama College of Engineering and Technology, AP, India.*

[5] *B.Tech, Student, Dept. of Electronics and Communication Engineering, Usha Rama College of Engineering and Technology, AP, India.*

Article DOI: https://doi.org/10.36713/epra16447
DOI No: 10.36713/epra16447

ABSTRACT

Due to the selective attenuation of light in water, underwater images are poorly visible and pose significant challenges in visual activities. The structural and statistical properties of different areas of degraded underwater images are damaged to different levels, resulting in an overall uneven drift of object representation and further degrading the image quality. In order to solve these problems, we introduce a method for enhancing underwater images through multi-bin histogram perspective equalization under to solve the problems caused by underwater images. We estimate the degree of feature variation in each image region by extracting the statistical features of the image and using this information to control feature enhancement to achieve adaptive feature enhancement, thereby improving the visual effect of degraded images. We first design a vibration model that exploits the difference between data elements and regular elements to improve the color correction performance of the linear transformation-based sub-interval method. In addition, a multiple threshold selection method was developed that adaptively selects a set of thresholds for interval division. Finally, a multi-bin sub-histogram equalization method is presented, which performs histogram equalization in each sub-histogram to improve image contrast. Underwater imaging experiments in various scenarios show that our method significantly outperforms many state-of-the-art methods in terms of quality and quantity.

INDEX TERMS: *Multiple intervals, multi-scale fusion (MF), sub histogram equalization (SHE), underwater image.*

I. INTRODUCTION

Many tasks, such as underwater welding and seabed investigation, require high-quality visual information, yet the complexity of the underwater environment makes obtaining clear underwater photographs challenging [1]. The structure and statistical features of several sections of a collected underwater image are altered. Damage at various levels is caused by selective attenuation based on light wavelength, resulting in uneven global drift in feature representation, as well as a reduction in the contrast and visibility of underwater images; thus, some improvements are required to extract meaningful information from it [2], [3]. Several strategies have been proposed to increase the quality of underwater photographs [4], [5], [6], [7], and [8].

However, most of them overlook the necessity of obtaining statistical information from images, resulting in distortion effects in the produced images. As a result, existing mature vision algorithms face considerable hurdles in meeting the desired performance for

SJIF Impact Factor (2024): 8.675| ISI I.F. Value: 1.241| Journal DOI: 10.36713/epra2016 ISSN: 2455-7838(Online)
EPRA International Journal of Research and Development (IJRD)
Volume: 9 | Issue: 4 | April 2024 - Peer Reviewed Journal

underwater picture augmentation. Several solutions have been developed to address underwater image deterioration. Histogram equalization (HE) is a popular method that offers the benefits of simple calculation and application. However, HE also has problems. For instance, it reduces information entropy (IE) and blurs details in an image. Given these limitations, some representative improvements have been proposed, including the sub histogram equalization (SHE) method [9], [10], [11], [12], [13], [14], [15], and [16].

The SHE approach outperforms HE in terms of image improvement. For example, brightness-preserving bi-histogram equalization [17] separates a histogram into two sub-histograms, with HE applied to each equal area. The dualistic sub image HE approach [18], which was based on SHE, divided a histogram using the original probability density function. Furthermore, Khan et al. [19] suggested a fuzzy double HE approach that employs the histogram's skewness to determine the segmentation threshold. These approaches, however, do not greatly improve underwater photographs since they ignore histogram properties. An image's histogram is typically used to describe the statistical distribution of the image's color. The degradation of underwater photos has a significant effect on the histogram.

To solve underwater image degradation, histograms should be assessed subjectively. Figure 1 depicts some example underwater photos, their polyline and 3-D histograms, and gradient frequency histograms. Polyline histograms graphically depict the histogram's trend and distribution, whereas 3-D histograms exhibit the image's color distribution more clearly. Observing both types of histograms reveals the three important properties of underwater photos.

Furthermore, the gradient frequency histograms of the underwater photos exhibit a left-skewed distribution. Light absorption, scattering, and underwater plankton all have an impact on underwater photographs, hence histograms are typically unequal in distribution, concentration, and deviation. These features then influence the quality of the underwater imaging process, resulting in deteriorated photos. This paper presents a novel underwater picture improvement method called multi-interval sub-histogram perspective equalization (UMSHE) for adjusting the histogram of underwater photos.

Problem Statement

Underwater imaging presents significant challenges due to the absorption, scattering, and attenuation of light in water. These challenges lead to poor visibility, low contrast, and color distortion in underwater images, hindering various applications such as underwater exploration, marine research, and surveillance. The goal of this project is to develop an effective image enhancement system specifically tailored for underwater images, aiming to improve visibility, contrast, and color accuracy. The proposed system should address the following key issues:

1. Low Visibility: Underwater environments often suffer from poor visibility due to factors like turbidity and depth. This results in hazy and blurred images with reduced contrast and detail.
2. Color Distortion: Light is absorbed and scattered differently across different wavelengths in water, causing color distortion in underwater images. The colors may appear washed out or skewed, making it difficult to accurately interpret the scene.
3. Low Contras: Absorption and scattering of light reduce the contrast between objects in underwater images. As a result, important details may be lost, and the overall quality of the image is compromised.
4. Noise and Artifacts: Underwater images are often plagued by noise and artifacts, further degrading image quality and making it challenging to extract meaningful information from the images.

The proposed image enhancement system should effectively tackle these challenges to produce clearer, more vibrant, and visually appealing underwater images. By improving image quality, the system aims to enhance the performance of various underwater imaging applications, including marine biology research, underwater inspection, and underwater archaeology. Additionally, the system should be computationally efficient and robust, capable of handling different underwater environments and conditions.

II. RELATED WORK

Three categories can be used to group existing underwater vision enhancement techniques: deep learning-based approaches, underwater picture enhancement techniques, and underwater image restoration techniques. A. Techniques for Restoring Underwater Images In order to recover image quality, underwater image restoration techniques seek to develop an efficient underwater image deterioration model [20]. Underwater optical imaging-based approaches [24], [25], [26]; polarisation characteristics-based methods [21], [22], [23]; and methods based on prior information [27], [28], [29], [30], [31] are examples of common techniques for restoring underwater images. The degree of polarisation of the background light in two or more photographs of the same scene was calculated by Treibitz and Schechner [21].

SJIF Impact Factor (2024): 8.675| ISI I.F. Value: 1.241| Journal DOI: 10.36713/epra2016 ISSN: 2455-7838(Online)
EPRA International Journal of Research and Development (IJRD)
Volume: 9 | Issue: 4 | April 2024 - Peer Reviewed Journal

In order to estimate the region's haze concentration and depth map, Chen et al. [22] suggested a region-specific estimation technique that made use of the dark channel prior (DCP).
By altering the transmittance of low polarisation, Hu et al. [23] recreated underwater images via transmittance correction. A Jaffe-McGlamery underwater optical image model was simplified by Trucco and Antillon [24] on the premise that forward scattering and homogeneous illumination have an impact on underwater images. By integrating underwater optical properties into the system response function, Hou et al. [25] were able to reconstruct images. A scene depth map was acquired by Song et al. [31], who then used a linear model to estimate the background light. The majority of restoration techniques can address certain issues with underwater image degradation, but their effectiveness is constrained by imprecise estimation of crucial model parameters and a failure to consider the impact of backscattering on optical imaging.

B. Underwater Image Enhancement Methods
Pixel intensity distribution adjustments are made in underwater picture enhancement techniques to improve photos. Spatial domain methods [32], [33], [34], transform domain methods [35], [36], [37], and fusion-based approaches [38], [39], [40] are among the frequently used techniques for underwater photos. To improve the photos, Iqbal et al. [32] extended the saturation (S) components in the Hue and the attenuated G B channel in the RGB colour model. In order to improve underwater photos, Fu et al. [33] suggested a two-step method for single underwater image enhancement (TS) that addressed two subproblems. In the RGB and CIE-Lab colour models, Huang et al. [34] developed relative global histogram stretching (RGHS). Amjad et al.'s [35] wavelet-based fusion technique addressed problems with poor contrast and colour shift. An efficient multiscale correlation wavelet approach (WB) for frequency domain image dehazing problems was presented by Liu et al. [36]. A wavelet-based perspective augmentation framework for underwater photos was proposed by Vasamsetti et al. [37]. Fusion weight maps were recently obtained from damaged underwater photos by Ancuti et al. [38].

All scene images undergo the same processing method, which may lead to an overabsorption or underabsorption of enhancement. The structural and statistical characteristics of underwater photographs are rarely taken into account by these methods, however this is something that has to change in the future.

C. Deep Learning Based Methods
Deep learning techniques are now applied to simple tasks. Recent deep learning techniques applied to underwater images can be categorised into dual generator generative adversarial networks based on the network architecture. However, because the network structure design and training data play a crucial role in the performance of deep learning-assisted approaches, the application breadth of these techniques remains restricted.

In the field of underwater image enhancement, various techniques and algorithms have been investigated to mitigate the challenges posed by underwater image conditions. Traditional methods typically include histogram equalization, contrast enhancement, and color correction to address issues such as poor visibility, color distortion, and low contrast. Advanced techniques include variants of adaptive histogram equalization (AHE), such as contrast-limited adaptive histogram equalization (CLAHE), which adaptively improves contrast and prevents over-amplification of noise. Recent advances include the integration of machine learning techniques such as deep neural networks for moe sophisticated, data-driven enhancement of underwater images. These methods aim to overcome the various challenges presented by underwater imaging conditions and pave the way for improved visual perception and analysis in underwater environments.

III. PROPOSED METHOD
Based on the structural and statistical characteristics of underwater images, a method for enhancing underwater images using perspective equalization of multi-interval subhistograms is proposed to address the problems caused by underwater images. The proposed method consists of color correction, contrast enhancement and multiscale fusion (MF). The flowchart of the detailed steps of the proposed method (see Fig. 2) is divided into three corresponding subgraphs. The various parts of the proposed method are described in detail below.

Color Correction
The suggested method creates a colour correction technique based on an SLVC to address the colour cast and improve the saturation of underwater photos. This technique creates a competitive relationship between the regular item and the data item of the variational model, processes the pixels directly, and eliminates the colour cast by extending and converting the pixels linearly. Lastly, SLVC can successfully adjust colour and increase image colour saturation. This technique can also improve the image's highlight details and is simple to use. The following are the process's primary steps.

SJIF Impact Factor (2024): 8.675| ISI I.F. Value: 1.241| Journal DOI: 10.36713/epra2016 ISSN: 2455-7838(Online)
EPRA International Journal of Research and Development (IJRD)
Volume: 9 | Issue: 4 | April 2024 - Peer Reviewed Journal

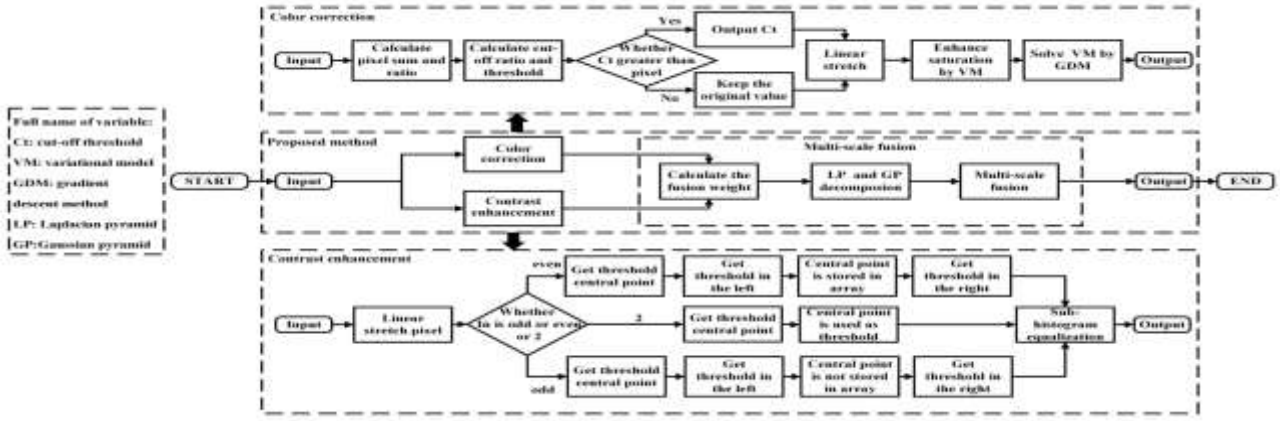

Fig.1 Flowchart of the detailed steps of the proposed method, which consists of three sub-processes: color correction, contrast enhancement and MF.

First, the pixel sum of a single channel is calculated with

$$S_c = \sum_{i=1}^{P \times Q} I_c(t)$$

Where, I stands for the input image, t for the pixel's grey level, c for the RGB picture's three channels, Ic(t) for the pixel value in channel c, and P for the number of rows in the modified matrix. supplied by the input picture The symbol Q stands for the quantity of columns, while Sc indicates the total number of pixels in a certain channel c. Next, the following formula is used to determine the ratio between each channel's maximum total pixel count and its total pixel count:

$$R_c = \frac{\mathrm{Max}\{S_R, S_G, S_B\}}{S_c}$$

Where, Rc is the ratio of the maximum total pixels to the total pixels of the particular channel c, and Max is the maximum value function. The channel is then divided into three sections using two cutoff ratios to get the cutoff thresholds. The following formulas are used to calculate the cutoff ratios:

$$\varpi_1^c = \theta_1 \times R_c$$

$$\varpi_2^c = \theta_2 \times R_c$$

Where, θ1 and θ2 are two constants in (0,1) and wc 1 and wc 2 stand for the cutoff ratios. As per [47] and the comprehensive experimental validation, θ1 and θ2 have values of 0.001 and 0.005, in that order. Next, using the lower quantile function, the cutoff levels for the linear transformation are established as follows:

$$e_1^c = \mathrm{F}\left(I_c(t), \varpi_1^c\right)$$

$$e_2^c = \mathrm{F}\left(I_c(t), \varpi_2^c\right)$$

Where, F is the lower quantile function and ec 1 and ec 2 stand for the cutoff criteria. While the second cutoff threshold returns pixel values more significant than the value of the second cutoff threshold, the pixel values replaced by the first cutoff threshold are smaller than the value of the first cutoff threshold. The following formula is used to get the pixel values and cutoff thresholds:

$$I_e^c(t) = \begin{cases} e_1^c & I_c(t) < e_1^c \\ e_2^c & I_c(t) > e_2^c \end{cases}$$

Where, Ic e (t) refers to the postprocessing pixel value. Then, the pixel values are stretched linearly using

SJIF Impact Factor (2024): 8.675| ISI I.F. Value: 1.241| Journal DOI: 10.36713/epra2016 ISSN: 2455-7838(Online)
EPRA International Journal of Research and Development (IJRD)
Volume: 9 | Issue: 4 | April 2024 - Peer Reviewed Journal

$$I_S^c(t) = \frac{I_e^c(t) - e_1^c}{e_1^c - e_2^c} \times 255$$

When a stretched pixel value is indicated by Ic S(t). In the end, a variational model with a data term and regularised terms is created to enhance saturation, taking inspiration from [48]. The data term penalises the difference between μ and Ic S(t), so as to keep the final image from deviating from the restored colour. Regularised terms widen the difference between the R, G, and B components as a way to improve saturation.

$$E(\mu_c) = \frac{1}{2}\sum_t \left(\begin{array}{l} \mu_c(t) - \\ I_S^c(t) \end{array} \right)^2 - \frac{\alpha}{2}\sum_t \left(\begin{array}{l} (\mu_c(t) - \mu_{c+1}(t))^2 \\ +(\mu_c(t) - \mu_{c+2}(t))^2 \end{array} \right)$$

Where, μc stands for the improved image; c is a 3-D space including the R, G, and B channels of the colour image (that is, R: c = 1, G: c = 2, and B: c = 3); and α is a positive parameter that regulates the regular term. By creating a competitive connection, data and regular elements are intended to modify the image's saturation and contrast.When a data item's competitive relationship with Subjective results and the R, G, and B channel histograms are arranged from left to right and a regular object reaches a point of energy minimization, the saturation and contrast are comparatively close to what is produced by visual effects used by humans. The minimizing process is carried out using the gradient descent method on the iterative computation results. The model's Euler-Lagrange derivative is computed as follows:

$$\delta E(\mu c) = (\mu c(t) - Ic\ S(t)) - \alpha(2\mu c - \mu c{+}1 - \mu c{+}2) = 0.$$

Then, above equation is solved using the gradient descent approach. The linearly stretched image serves as the starting point for solving below equation.

$$\frac{\partial \mu}{\partial m} = -\delta E(u)$$

Where, m denotes the timeline of iterative calculations. Then, the above equation is discretized and rewritten as follows:

$$\frac{\mu_c^{k+1}(t) - \mu_c^k(t)}{\Delta m} = \left(\begin{array}{l} I_S^c(t) - \\ \mu_c^k(t) \end{array} \right) + \alpha \left(\begin{array}{l} 2\mu_c^k(\boldsymbol{t}) - \mu_{c+1}^k(t) \\ -\mu_{c+2}^k(t) \end{array} \right)$$

Where, k is the number of calculations made in iteration. Following a straightforward left-right identity transformation of below equation, the following is the iteration rule obtained:

$$\mu_c^{k+1} = \mu_c^k(1 - \Delta m(1 - 2\alpha)) + \Delta m\left(I_S^c - \alpha\mu_{c+1}^k - \alpha\mu_{c+2}^k\right)$$

Where, $0 < \Delta m \leq 1/(1 - 2\alpha)$.

The white balance (AWB) method and the subinterval linear transformation (SLC) method are two two-color correction techniques that are chosen in order to compare and evaluate the efficacy of the SLVC approach. It is possible to determine that the SLVC approach produces better colour correction effects and that the histogram works steadily by comparing the subjective outcomes of various methods with the corresponding three-channel histograms discussed in results section.

SJIF Impact Factor (2024): 8.675| ISI I.F. Value: 1.241| Journal DOI: 10.36713/epra2016 ISSN: 2455-7838(Online)
EPRA International Journal of Research and Development (IJRD)
Volume: 9 | Issue: 4 | April 2024 - Peer Reviewed Journal

B. Contrast Enhancement

The contrast level of an underwater image has a big impact on the quality and details of the image. Low contrast and blurry details remain concerns even when the SLVC algorithm fixes saturation deterioration and colour casting. Thus, in order to address the poor contrast and fuzzy features of underwater images, this study suggests using the MSHE approach. The MSHE method performs HE by splitting a histogram into several sub histograms. The HE is more effective and the histogram correction is superior when several sub histograms are divided and processed. Furthermore, the MSHE technique improves visual contrast without noise and artefacts. The following are the MSHE method's primary steps.

Step 1: Pixel stretching: Because of the diversity of pixel sizes of the supplied underwater images, preprocessing is required. Thus, the following linear stretching operation is performed to ensure that the pixel values are all within [0, 255]:

$$H_c(x) = \frac{(I_c(t) - mi_c)}{(ma_c - mi_c)} \times 255$$

where mac and mic stand for the maximum and minimum pixel values of a single channel image, respectively, and Hc(t) indicates the pixel value following linear stretching. Ic(t) represents the pixel value of the starting image at a specific time.

Step 2: Selecting the interval division threshold The interval division criteria that split the histogram into several sub histograms must be established in order to use the MSHE approach. Using the lower quantile approach, a central threshold point (Cp) for the entire histogram is first found. Then, for interval division, a number of thresholds are chosen around the Cp. The statistically lower quantile, which falls between [0.75, 0.8], is the selection criterion used for Cp. This criterion takes into account all of the features of the image gra

dient frequency histogram's left-skewed distribution.

The fraction of the modest gradient value is significant, and the significant gradient value is tiny, according to the objective law of the picture gradient. A tiny gradient value's interval can be represented by this portion of the interval if the cumulative distribution function's value falls between [0.75, 0.8].

Consequently, the gradient image is divided into large and small gradient parts by the lower quantile limit, which utilises 0.75. It is necessary to equalise the large gradient portion due to its excessively low pixel count, and the tiny gradient portion due to its excessively high pixel count. Consequently, the picture histogram is divided into two sections that require the greatest adjustment using the value that is produced using the lower quantile approach as Cp. Image processing performance is best, according, when the threshold is chosen on both sides of the central point. Numerous experiments also support the appropriateness of this threshold selection. .

When a threshold selection process is carried out, the left and right thresholds are chosen. The product of b times the pixel value variance and the number of times the threshold operation is used to produce all thresholds are then subtracted or added using Cp. The interval division threshold array has 256 as the last item and 0 as the first item. An even number of interval thresholds is required when Ni is odd. Consequently, Cp is only utilised to calculate the other thresholds and is not used as one of the thresholds itself. Ni is used to determine the threshold operation to use. When Ni is even, the threshold calculation procedure is the same on both sides of Cp. A schematic diagram of the threshold selection method is shown in Fig. 4, where Cp represents the central point, Ni denotes the number of thresholds, d indicates the threshold, and n indicates the number of intervals (i.e., Ni is to the left of Cp when Ni is even and Ni is to the left of Cp when it is odd). To select Cp, the number and frequency of the occurrence of each pixel value in the input image are calculated as follows:

$$N = \text{imhist}(H_c(t))$$

$$h = \frac{N}{P \times Q}$$

C. Multi-Scale Fusion

MF is used to combine the results of contrast enhancement and colour correction, giving each section of the final image a unique appearance based on the input sequence. While most image enhancement techniques have some drawbacks, MF using weight map features may pick the right pixels from each input image and combine them to create a final image. The ability of MF to consistently enhance underwater images using multiscale strategies—even in the absence of prior distance map estimation—is a crucial benefit. Furthermore, the outcomes of the enhancing procedure can be effectively maintained.

SJIF Impact Factor (2024): 8.675| ISI I.F. Value: 1.241| Journal DOI: 10.36713/epra2016 ISSN: 2455-7838(Online)
EPRA International Journal of Research and Development (IJRD)
Volume: 9 | Issue: 4 | April 2024 - Peer Reviewed Journal

1) Weight Map: Each input image's contrast, exposure, and saturation weights are determined, and the resulting weight maps are combined to create an aggregated weight map. Next, the total weight is adjusted by adding the total of

$$W = F_C \times F_S \times F_E$$

$$\overline{W} = \left[\sum_{t'=1}^{k} W\right]^{-1} W$$

Where, FC, FE, and FS stand for the feature a weight of contrast, exposure, and saturation, respectively, and W denotes the aggregated weight map. W stands for the aggregated weight map that has been normalised, and k is the number of input photos.

2) Fusion: MF uses a multi-scale approach based on Laplacian and Gaussian pyramids to fuse the weight map with the input map pixel by pixel. The input image is filtered using a low pass Gaussian kernel at each layer by the Gaussian pyramid, which then breaks the image down into the sum of the band pass images. The pyramids of the decomposed input map and weight map are at a consistent level when multi-scale decomposition is finished, and the maps are fused pixel by pixel and reassembled into a
into a final image. The equation is as follows:

$$R_l(x) = \sum_{t=1}^{k} G_l\left\{\overline{W}_t\right\} L_l\{I\}$$

where Rl(x) represents the reconstructed result image, Gl{W¯ t} denotes the Gaussian pyramid decomposed from the weight map, and Ll{I} represents the Laplacian pyramid decomposed from the input image.

IV . RESULT AND DISCUSSION

An ablation experiment, a runtime evaluation, a qualitative evaluation, and a quantitative evaluation are used to assess the underwater image quality produced by the suggested method. Instruments are used in the qualitative evaluation to watch the image or run experiments with repeated observation. After that, a number of testers assess and examine the image quality. Using mathematical techniques, the quantitative assessment computes the image's objective evaluation index and uses the computed data to determine the image's quality. Ten example methods are chosen for this study, and they are contrasted with the suggested way. There are two deep learning methods, four restoration methods, and four enhancement approaches in total.

.

SJIF Impact Factor (2024): 8.675| ISI I.F. Value: 1.241| Journal DOI: 10.36713/epra2016 ISSN: 2455-7838(Online)
EPRA International Journal of Research and Development (IJRD)
Volume: 9 | Issue: 4 | April 2024 - Peer Reviewed Journal

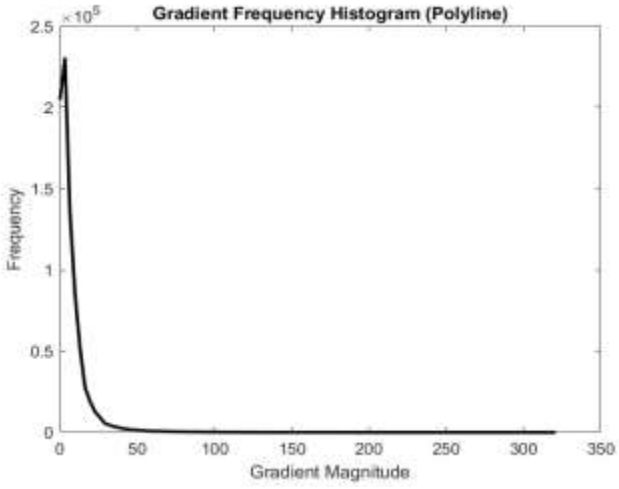

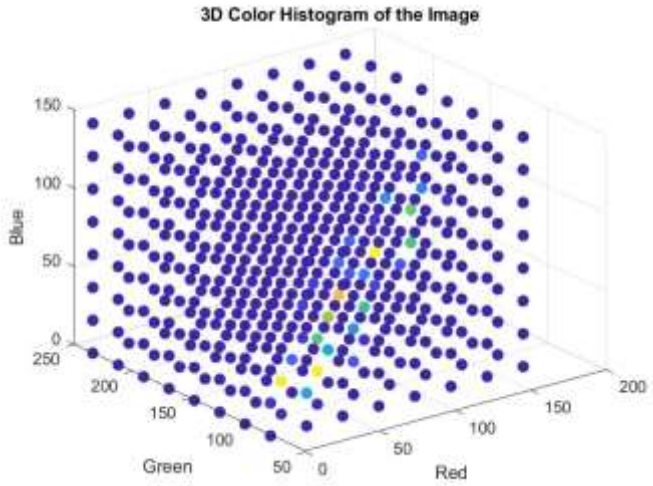

Original Underwater Image:
The original underwater image that was imported from the file is this one. It acts as the catalyst for the process of improvement. 3D RGB colour space histogram of the original image: This illustration shows a 3D histogram of the RGB colour space. The intensity of the plotted dots indicates the frequency of occurrence of each color channel (Red, Green, and Blue), which is represented by an axis.

Polyline with Gradient Frequency Histogram: The gray scale version of the original image's gradient magnitudes is displayed in this graphic as their frequency distribution. It sheds light on how edge strengths or picture gradients are distributed.

Original UNDERWATER Image
This is the original underwater image converted to grayscale.

Thresholding with color correction
This figure shows the result of applying a thresholding technique with color correction. It might be a pre-processing step for enhancing image features or improving overall image quality.

DCP (Histogram Equalization
This figure displays the result of applying histogram equalization, specifically Contrast Limited Adaptive Histogram Equalization (CLAHE) on the input image. It enhances the image's contrast and overall brightness.

SJIF Impact Factor (2024): 8.675| ISI I.F. Value: 1.241| Journal DOI: 10.36713/epra2016 ISSN: 2455-7838(Online)
EPRA International Journal of Research and Development (IJRD)
Volume: 9 | Issue: 4 | April 2024 - Peer Reviewed Journal

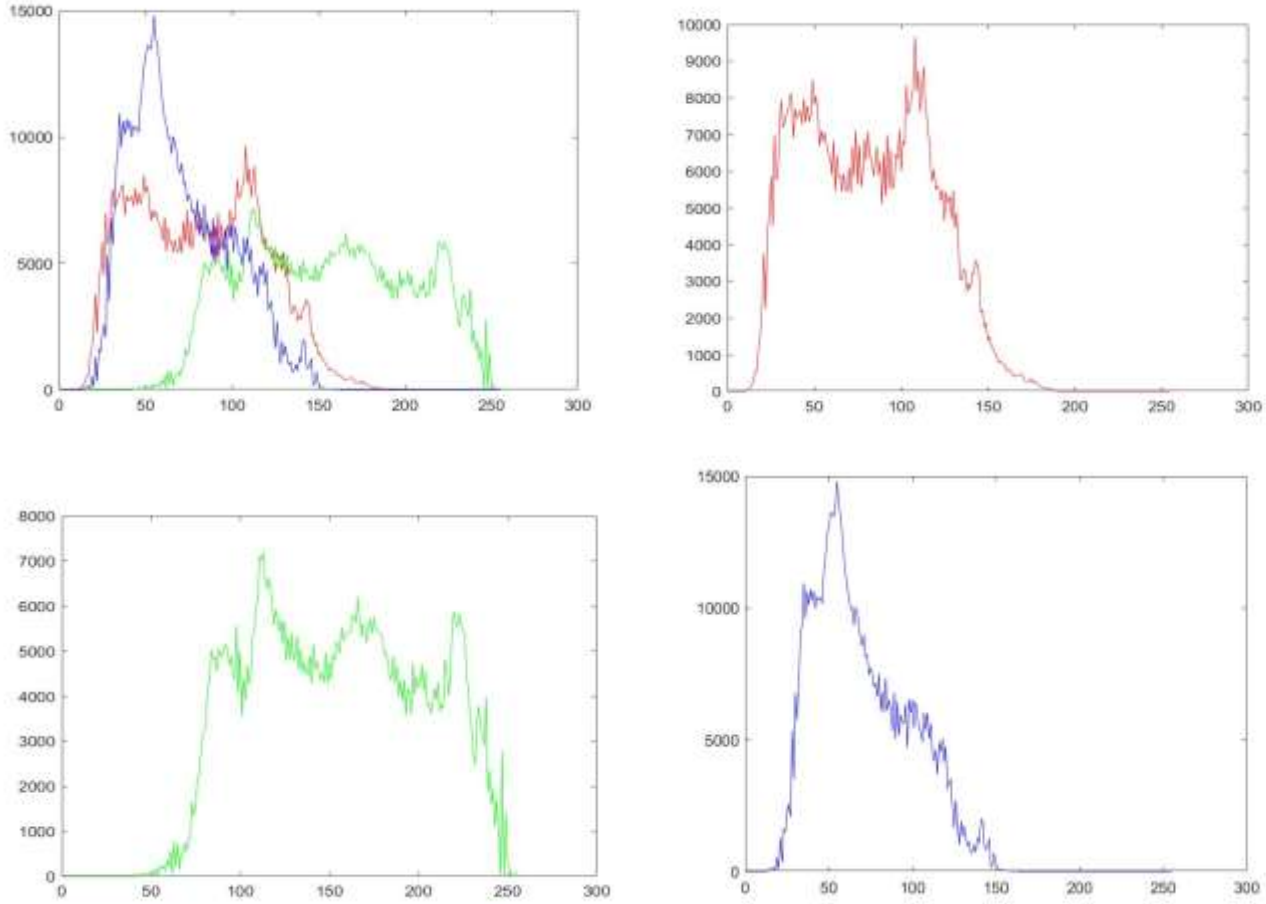

Histograms of RGB Channels
These plots show the histogram distribution of pixel intensities for each RGB channel separately. It helps visualize the distribution of colors in the image.

ICM Technique
This image demonstrates the result of applying the Iterative Contrast Modification (ICM) technique. It's a method used for enhancing image contrast and improving visual quality.

Color Channel Correction
This figure represents the result of color channel correction, possibly adjusting color balance or removing color casts in the image.

Red Compensated
This image shows the result after compensating for the red channel. It might be part of a color correction process to balance color channels.

SLVC (White Balancing)
This image displays the result of applying White Balancing, aiming to adjust the overall color cast and improve color accuracy.

MSHE (Gamma Correction)
This image illustrates the result of Gamma Correction. It adjusts the brightness and contrast of the image by applying a gamma function.

SJIF Impact Factor (2024): 8.675| ISI I.F. Value: 1.241| Journal DOI: 10.36713/epra2016 ISSN: 2455-7838(Online)
EPRA International Journal of Research and Development (IJRD)
Volume: 9 | Issue: 4 | April 2024 - Peer Reviewed Journal

UMSHE-image enhancement

This image shows the result after sharpening the image using an appropriate image enhancement technique.

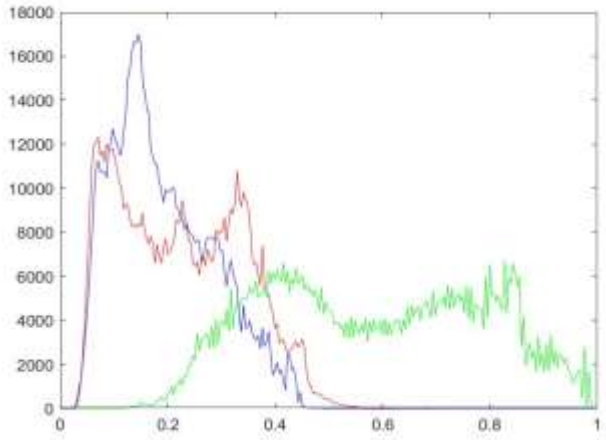

SJIF Impact Factor (2024): 8.675| ISI I.F. Value: 1.241| Journal DOI: 10.36713/epra2016 ISSN: 2455-7838(Online)
EPRA International Journal of Research and Development (IJRD)
Volume: 9 | Issue: 4 | April 2024 - Peer Reviewed Journal

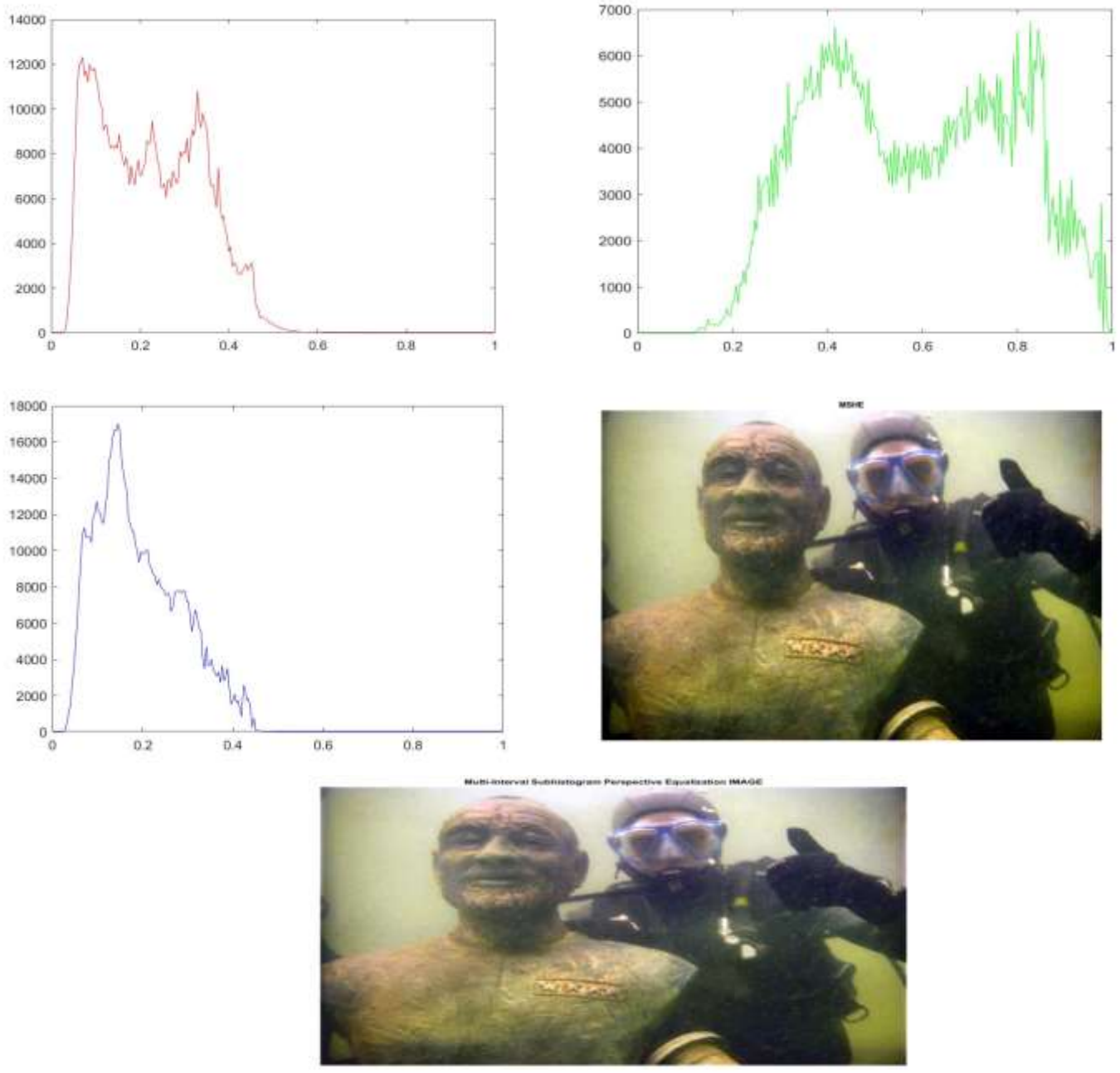

Fig Final Enhanced Image

Multi-Interval Sub histogram Perspective Equalization Image:

After using the Multi-Interval Subhistogram Perspective Equalisation approach, the final improved image looks like this. It enhances visual appeal, contrast, and image quality by combining several enhancement techniques. The goal of the image enhancement process is to increase the overall quality and visual look of the original underwater image, and each of these output images reflects a stage or combination of steps in that process.

Analysis of the results obtained:

Mean: The mean intensity value of the enhanced image is 0.4594. This gives an indication of the average brightness level of the image.

SJIF Impact Factor (2024): 8.675| ISI I.F. Value: 1.241| Journal DOI: 10.36713/epra2016 ISSN: 2455-7838(Online)
EPRA International Journal of Research and Development (IJRD)
Volume: 9 | Issue: 4 | April 2024 - Peer Reviewed Journal

Entropy: The entropy of the enhanced image is 7.7820. Entropy represents the amount of uncertainty or randomness in the image intensity values. Higher entropy indicates more diversity in pixel intensities.

RMS (Root Mean Square): The RMS value for each channel of the image is calculated, indicating the root mean square contrast of the image. A higher RMS value suggests higher contrast.

MSE (Mean Square Error): The Mean Square Error between the enhanced image and the original grayscale image is calculated for each channel. It quantifies the average squared difference between the pixels of the two images. Lower MSE values indicate better similarity between the images.

Image Contrast: The contrast of the image is measured, which is essentially the difference between the maximum and minimum pixel values. Here, the contrast is reported as 0, which might indicate a low contrast image.

SSIM (Structural Similarity Index): SSIM measures the similarity between two images. A value closer to 1 indicates high similarity. Here, SSIM is reported as 0.012526, which might indicate a significant difference between the enhanced and original images.

AG (Average Gradient): AG measures the average gradient magnitude of the image. It is calculated using the Sobel operator. A higher AG suggests a higher amount of image detail.

PCQI (Perceptual Contrast Quality Index): PCQI measures the perceptual quality of the image. Higher PCQI values indicate better image quality.

UCIQE (Universal Image Quality Index): UCIQE is another metric for assessing image quality. Higher UCIQE values indicate better image quality.

Each of these metrics provides different insights into the quality and characteristics of the enhanced image. Together, they help in understanding various aspects such as brightness, contrast, similarity to the original image, and overall visual quality.

Elapsed time is 5.313565 seconds.
Mean =0.4594
Entropy = 7.7820
RMS = 0.5124
MSE =(:,:,1) =0.0340
(:,:,2) = 0.0451
(:,:,3) = 0.0146
image_contrast = 0
SSIM= 0.012526
AG = Inf
PCQI= 0.4303
UCIQE= 0.5407

V. CONCLUSION

This study introduces a novel approach for enhancing underwater images by estimating feature drift across different image regions and leveraging this information to guide enhancement processes. The method begins by estimating the statistical characteristics of the image histograms, specifically tailored for underwater imagery. It then proposes a combined enhancement technique involving color correction and Multi-Scale Histogram Equalization (MSHE). The color correction method, SLVC, targets color cast issues and enhances saturation by employing a variational model for processing, thereby achieving better and more reasonable results. MSHE is subsequently applied to improve contrast and detail information by dividing histograms into multiple intervals and equalizing them separately. Finally, the resulting enhanced images are fused using a fusion technique, resulting in a visually improved final image. Both qualitative and quantitative evaluations demonstrate the effectiveness of the proposed method in addressing color cast, enhancing saturation, contrast, and detail information. Additionally, the method extends Histogram Equalization (HE) to any number of intervals, enhancing its adaptability and performance. While the method shows promise, it still has limitations, such as potential red shading in deep-sea images and a lack of consideration for different underwater scenes and depths. To address these shortcomings, future work will focus on refining

SJIF Impact Factor (2024): 8.675| ISI I.F. Value: 1.241| Journal DOI: 10.36713/epra2016 ISSN: 2455-7838(Online)
EPRA International Journal of Research and Development (IJRD)
Volume: 9 | Issue: 4 | April 2024 - Peer Reviewed Journal

the method to selectively enhance image areas, considering varying scene depths, and adapting enhancement levels to changes in light and depth.

REFERENCES

1. *Z. Jiang, Z. Li, S. Yang, X. Fan, and R. Liu, "Target oriented perceptual adversarial fusion network for underwater image enhancement," IEEE Trans. Circuits Syst. Video Technol., vol. 32, no. 10, pp. 6584–6598, Oct. 2022, doi: 10.1109/TCSVT.2022.3174817.*
2. *P. Zhuang, C. Li, and J. Wu, "Bayesian retinex underwater image enhancement," Eng. Appl. Artif. Intell., vol. 101, 2021, Art. no. 104171, doi: 10.1016/j.engappai.2021.104171.*
3. *R. Liu, Z. Jiang, S. Yang, and X. Fan, "Twin adversarial contrastive learning for underwater image enhancement and beyond," IEEE Trans. Image Process., vol. 31, pp. 4922–4936, 2022, doi: 10.1109/TIP.2022.3190209.*
4. *W. Ren, J. Pan, H. Zhang, X. Cao, and M. H. Yang, "Single image dehazing via multi-scale convolutional neural networks with holistic edges," Int. J. Comput. Vis., vol. 128, no. 1, pp. 240–259, 2020 doi: 10.1007/s11263-019-01235-8.*
5. *S. Anwar and C. Li, "Diving deeper into underwater image enhancement: A survey," Signal Process., Image Commun., vol. 89, Nov. 2020, Art. no. 115978, doi: 10.1016/j.image.2020.115978.*
6. *J. Zhou, T. Yang, W. Ren, D. Zhang, and W. Zhang, "Underwater image restoration via depth map and illumination estimation based on single image," Opt. Exp., vol. 29, no. 19, pp. 29864–29886, 2021, doi: 10.1364/OE.427839.*
7. *C. Li, S. Anwar, J. Hou, R. Cong, C. Guo, and W. Ren, "Underwater image enhancement via medium transmission-guided multi-color space embedding," IEEE Trans. Image Process., vol. 30, pp. 4985–5000, 2021, doi: 10.1109/TIP.2021.3076367.*
8. *J. Zhou, T. Yang, and W. Zhang, "Underwater vision enhancement technologies: A comprehensive review, challenges, and recent trends," Appl. Intell., vol. 52, pp. 1–28, 2022, doi: 10.1007/s10489-022-03767-y.*
9. *T. Li, Q. Yang, S. Rong, L. Chen, and B. He, "Distorted underwater image reconstruction for an autonomous underwater vehicle based on a self-attention generative adversarial network," Appl. Opt., vol. 59, no. 32, pp. 10049–10060, 2020, doi: 10.1364/AO.402024.*
10. *X. Ding, Z. Liang, Y. Wang, and X. Fu, "Depth-aware total variation regularization for underwater image dehazing," Signal Process., Image Commun., vol. 98, 2021, Art. no. 116408, doi: 10.1016/j.image.2021.116408.*
11. *T. Li et al., "Underwater image enhancement framework using adaptive color restoration and dehazing," Opt. Express, vol. 30, no. 4, pp. 6216–6235, 2022, doi: 10.1364/OE.449930.*
12. *J. Zhou, D. Zhang, W. Ren, and W. Zhang, "Auto color correction of underwater images utilizing depth information," IEEE Geosci. Remote Sens. Lett., vol. 19, 2022, Art. no. 1504805, doi: 10.1109/LGRS.2022.3170702.*
13. *J. Zhou, T. Yang, W. Chu, and W. Zhang, "Underwater image restoration via backscatter pixel prior and color compensation," Eng. Appl. Artif. Intell., vol. 111, 2022, Art. no. 104785, doi: 10.1016/j.engappai.2022.104785.*
14. *P. Zhuang, J. Wu, F. Porikli, and C. Li, "Underwater image enhancement with hyper-laplacian reflectance priors," IEEE Trans. Image Process., vol. 31, pp. 5442–5455, 2022, doi: 10.1109/TIP.2022.3196546.*
15. *J. Zhou, D. Zhang, and W. Zhang, "Classical and state-of-the-art approaches for underwater image defogging: A comprehensive survey," Front. Inf. Technol. Electron. Eng., vol. 21, no. 5, pp. 1745–1769, 2020, doi: 10.1631/FITEE.2000190.*
16. *Y. Guo, H. Li, and P. Zhuang, "Underwater image enhancement using a multiscale dense generative adversarial network," IEEE J. Ocean. Eng., vol. 45, no. 3, pp. 862–870, Jul. 2020, doi: 10.1109/JOE.2019.2911447.*
17. *Y.-T. Kim, "Contrast enhancement using brightness preserving bihistogram equalization," IEEE Trans. Consum. Electron., vol. 43, no. 1, pp. 1–8, Feb. 1997, doi: 10.1109/30.580378.*
18. *Y. Wang, Q. Chen, and B. Zhang, "Image enhancement based on equal area dualistic sub-image histogram equalization method," IEEE Trans. Consum. Electron., vol. 45, no. 1, pp. 68–75, Feb. 1999, doi: 10.1109/30.754419.*
19. *M. F. Khan, D. Goyal,M.M. Nofal, E. Khan, R. Al-Hmouz, and E. HerreraViedma, "Fuzzy-based histogram partitioning for bi-histogram equalization of low contrast images," IEEE Access, vol. 8, pp. 11595–11614, 2020, doi: 10.1109/ACCESS.2020.2965174.*
20. *H.-H. Chang, C.-Y. Cheng, and C.-C. Sung, "Single underwater image restoration based on depth estimation and transmission compensation," IEEE J. Ocean. Eng., vol. 44, no. 4, pp. 1130–1149, Oct. 2019, doi: 10.1109/JOE.2018.2865045.*
21. *T. Treibitz and Y. Y. Schechner, "Active polarization descattering," IEEE Trans. Pattern Anal. Mach. Intell., vol. 31, no. 3, pp. 385–399, Mar. 2009, doi: 10.1109/TPAMI.2008.85.*
22. *Z. Chen, H. Wang, J. Shen, X. Li, and L. Xu, "Regionspecialized underwater image restoration in inhomogeneous optical environments," Optik, vol. 125, no. 9, pp. 2090–2098, May 2014, doi: 10.1016/j.ijleo.2013.10.038.*
23. *H. Hu, L. Zhao, B. Huang, X. Li, H. Wang, and T. Liu, "Enhancing visibility of polarimetric underwater image by transmittance correction," IEEE Photon. J., vol. 9, no. 3, Jun. 2017, Art. no. 6802310, doi: 10.1109/JPHOT.2017.2698000.*
24. *E. Trucco and A. T. Olmos-Antillon, "Self-tuning underwater image restoration," IEEE J. Ocean. Eng., vol. 31, no. 2, pp. 511–519, Apr. 2006, doi: 10.1109/JOE.2004.836395.*
25. *W. Hou, D. J. Gray, A. D. Weidemann, G. R. Fournier, and J. L. Forand, "Automated underwater image restoration and retrieval of related optical properties," in Proc. IEEE Int. Geosci. Remote Sens. Symp., 2007, pp. 1889–1892, doi: 10.1109/IGARSS.2007.4423193.*
26. *M. Boffety, F. Galland, and A. G. Allais, "Color image simulation for underwater optics," Appl. Opt., vol. 51, no. 23, pp. 5633–5642, 2012, doi: 10.1364/AO.51.005633.*

SJIF Impact Factor (2024): 8.675| ISI I.F. Value: 1.241| Journal DOI: 10.36713/epra2016 ISSN: 2455-7838(Online)
EPRA International Journal of Research and Development (IJRD)
Volume: 9 | Issue: 4 | April 2024 - Peer Reviewed Journal

27. *K. He, J. Sun, and X. Tang, "Single image haze removal using dark channel prior," IEEE Trans. Pattern Anal. Mach. Intell., vol. 33, no. 12, pp. 2341–2353, Dec. 2011, doi: 10.1109/TPAMI.2010.168.*
28. *P. Drews, E. Nascimento, F. Moraes, S. Botelho, and M. Campos, "Transmission estimation in underwater single images," in Proc. IEEE Int. Conf. Comput. Vis. Workshops, 2013, pp. 825–830, doi: 10.1109/ICCVW.2013.113.*
29. *Y.-T. Peng and P. C. Cosman, "Underwater image restoration based on image blurriness and light absorption," IEEE Trans. Image Process., vol. 26, no. 4, pp. 1579–1594, Apr. 2017, doi: 10.1109/TIP.2017. 2663846.*
30. *[30] C.-Y. Li, J.-C. Guo, R.-M. Cong, Y.-W. Pang, and B. Wang, "Underwater image enhancement by dehazing with minimum information loss and histogram distribution prior," IEEE Trans. Image Process., vol. 25, no. 12, pp. 5664–5677, Dec. 2016, doi: 10.1109/TIP.2016.2612882.*
31. *[31] W. Song, Y. Wang, D. Huang, and D. Tjomdronegoro, "A rapid scene depth estimation model based on underwater light attenuation prior for underwater image restoration," Pac. Rim Conf. Multimedia, vol. 11164, pp. 678–688, 2018, doi: 10.1007/978-3-030-00776-8_62.*
32. *[32] K. Iqbal, R. A. Salam, A. Osman, and A. Z. Talib, "Underwater image enhancement using an integrated color model," IAENG Int. J. Comput. Sci., vol. 34, no. 2, p. 12, 2007.*
33. *[33] X. Fu, Z. Fan, M. Ling, Y. Huang, and X. Ding, "Two-step approach for single underwater image enhancement," in Proc. Int. Symp. Intell. Signal Process. Commun. Syst., 2017, pp. 789–794, doi: 10.1109/ISPACS.2017.8266583.*
34. *[34] D. Huang, Y. Wang, W. Song, J. Sequeira, and S. Mavromatis, "Shallowwater image enhancement using relative global histogram stretching based on adaptive parameter acquisition," in Proc. Int. Conf. Multimedia Model., 2018, pp. 453–465, doi: 10.1007/978-3-319-73603-7_37.*
35. *[35] A. Khan, A. S. Ali, A. S. Malik, A. Anwer, and F. Meriaudeau, "Underwater image enhancement by wavelet-based fusion," in Proc. IEEE Int. Conf. Underwater Syst. Technol., Theory Appl., 2016, pp. 83–88, doi: 10.1109/USYS.2016.7893927.*
36. *[36] X. Liu, H. Zhang, Y. Cheung, X. You, and Y. Tang, "Efficient single image dehazing and denoising: An efficient multi-scale correlated wavelet approach," Comput. Vis. Image Understanding, vol. 162, pp. 23–33, Sep. 2017, doi: 10.1016/j.cviu.2017.08.002.*
37. *[37] S. Vasamsetti, N. Mittal, B. C. Neelapu, and H. K. Sardana, "Wavelet based perspective on variational enhancement technique for underwater imagery," Ocean Eng., vol. 141, pp. 88–100, Sep. 2017, doi: 10.1016/j.oceaneng.2017.06.012.*
38. *[38] C. Ancuti, C. O. Ancuti, T. Haber, and P. Bekaert, "Enhancing underwater images and videos by fusion," in Proc. IEEE Conf. Comput. Vis. Pattern Recognit., 2012, pp. 81–88, doi: 10.1109/CVPR.2012.6247661.*
39. *[39] C. O. Ancuti, C. Ancuti, C. De Vleeschouwer, and P. Bekaert, "Color balance and fusion for underwater image enhancement," IEEE Trans. Image Process., vol. 27, no. 1, pp. 379–393, Jan. 2018, doi: 10.1109/TIP.2017.2759252.*